Comparative Study of Turbo Equalization Schemes Using Convolutional, Convolutional Turbo, and Block-Turbo Codes

Bee Leong Yeap, Tong Hooi Liew, J. Hámorský, and Lajos Hanzo, *Senior Member, IEEE*

***Abstract*—Turbo equalizers have been shown to be successful in mitigating the effects of inter-symbol interference introduced by partial response modems and by dispersive channels for code rates of $R \leqslant 1/2$. In this contribution, we comparatively studied the performance of a range of binary phase-shift keying turbo equalizers employing block-turbo codes, namely Bose–Chaudhuri–Hocquenghen turbo codes, convolutional codes, and convolutional turbo codes having high code rates, such as $R = 3/4$ and $R = 5/6$, over a dispersive five-path Gaussian channel and an equally weighted symbol-spaced five-path Rayleigh fading channel. These turbo equalization schemes were combined with an iterative channel estimation scheme in order to characterize a realistic scenario. The simulation results demonstrated that the turbo-equalized system using convolutional turbo codes was the most robust system for all code rates investigated.**

***Index Terms*—Bose–Chaudhuri–Hocquenghen codes, convolutional codes, iterative decoding, iterative equalization, joint equalization and decoding, turbo codes, turbo decoding, turbo equalization.**

I. Introduction

Turbo equalization (TEQ) [1] was proposed by Douillard *et al.* in 1995 for a rate $R = 1/2$ convolutional-coded binary phase-shift keying (BPSK) system. Specifically, Douillard *et al.* demonstrated that the turbo equalizer was capable of mitigating the effects of inter-symbol interference (ISI), provided that the channel impulse response (CIR) was known. Here the performance improvements were obtained by performing the channel equalization and channel decoding iteratively. Gertsman and Lodge [2] then showed that the turbo principle can compensate for the performance degradations due to imperfect CIR estimation. Different iteration termination criteria [3], such as cross-entropy minimization [4], were also investigated in order to minimize the number of iterations carried out by the turbo equalizer. A turbo equalization scheme was proposed by Bauch and Franz [5] for the global system for mobile communications (GSM) where different approaches of overcoming the dispersion of the so-called *a priori* information due to the interburst interleaving scheme were investigated. Research into combined $R = 1/3$ convolutional turbo coding [6], [7] and iterative channel equalization has also been conducted by Raphaeli and Zarai [8]. Their results showed that for BPSK systems transmitting over nonrecursive channels the turbo equalizer using turbo codes outperformed the turbo equalizer utilizing convolutional codes. In the context of recursive channels, such as precoded magnetic storage media [9], the same trend was observed in the "floor" region of the bit-error rate (BER) curve. However, in the "cliff" region, the opposite trend was observed, where the turbo equalizer employing convolutional codes outperformed the turbo equalizer using turbo codes.

With the ever increasing demand for bandwidth, current systems aim to increase the spectral efficiency by invoking high-rate codes. This has been the motivation for research into block-turbo codes, which have been shown by Hagenauer *et al.* [10] to outperform convolutional turbo codes using punctured high-rate convolutional component codes, when the coding rate is higher than $R = 2/3$. It was also observed that a rate $R = 0.981$ block turbo code using BPSK over the nondispersive Gaussian channel can operate within 0.27 dB of the Shannon limit [11]. Another method of generating high-rate turbo codes have been proposed by Açikel and Ryan [12], whereby a rate $R = 1/3$ turbo code consisting of two $R = 1/2$ convolutional codes is punctured. These high-rate turbo codes have been shown to perform better than the turbo codes proposed by Hagenauer *et al.* [10]. The puncturing patterns were optimized for transmission over the nondispersive additive white Gaussian noise (AWGN) channel.

In this contribution, our objective is to investigate the performance of BPSK turbo equalizers employing different classes of high-rate codes, namely $R = 3/4$ and $R = 5/6$ convolutional codes, convolutional turbo codes, and block—turbo codes. This is because known turbo equalization results have only been presented for turbo equalizers using convolutional codes and convolutional turbo codes for code rates of $R = 1/3$ and $R = 1/2$ [1], [8]. Specifically, Bose–Chaudhuri–Hocquengham (BCH) codes [13], [14] are used as the component codes of the BT codec. Since BCH codes can be constructed with parameters n and k, which represent the number of coded bits and data bits, respectively, we will use the notation BCH (n, k). The notations convolutional coded (CC), convolutional turbo (CT), and block-turbo (BT), will also be used to represent the CC system, the convolutional turbo coded scheme, and the BCH turbo coded system, respectively.

The organization of this paper is as follows. In Section II, the model of the investigated systems is described. Subsequently, an

Manuscript received September 23, 1999; revised August 2, 2000 and June 7, 2001; accepted July 18, 2001. The editor coordinating the review of this paper and approving it for publication is D. L. Goeckel. This work was supported in part by the Commission of European Community and in part by the Engineering and Physical Sciences Research Council (EPSRC), U.K.

The authors are with the Department of Electronics and Computer Science, University of Southampton, Southampton, U.K. (e-mail: bly@ecs.soton.ac.uk; lh@ecs.soton.ac.uk).

Publisher Item Identifier S 1536-1276(02)02928-8.

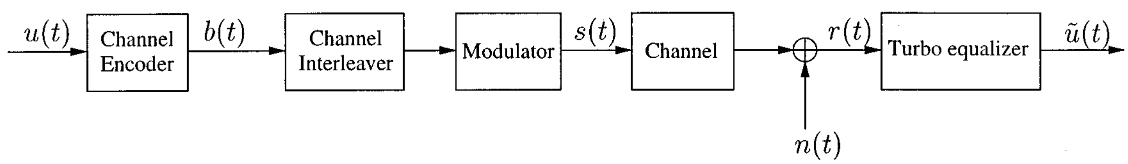

Fig. 1. A coded BPSK system employing a turbo equalizer at the receiver.

overview of turbo equalization [27] is presented in Section III. Section IV discusses the relative complexity of the turbo equalizers, while Section V presents the simulation parameters. The performance of the systems is demonstrated in Section VI and, finally, we conclude in Section VII.

II. System Overview

In our investigations, we have considered a coded BPSK system employing turbo equalization [27] at the receiver, as illustrated in Fig. 1. At the transmitter, the source bits u_k are encoded in order to yield the coded bits b_k. Three classes of codecs are investigated, namely convolutional codecs, the convolutional turbo codecs, and the BCH turbo codecs for code rates of $R \approx 0.5$, $R \approx 0.75$, and $R \approx 0.83$. Subsequently, the coded bits are channel-interleaved and passed to the modulator, which produces the modulated signal $s(t)$, transmitted in bursts.

The transmission burst structure used in this system is the Frames Mode A1 (FMA1) nonspread burst as specified in the Pan-European FRAMES proposal [15]. It consists of a 27-symbol training sequence, which separates two 72-symbol data sequences. At each end of the transmission burst, there are three tail symbols. The signal $s(t)$ is transmitted over the channel characterized by the CIR $h(t)$ and further corrupted by the zero-mean complex white Gaussian noise $n(t)$, having a variance of $\sigma^2 = N_0/2$, where N_0 is the single-sided noise power spectral density at the receiver, yielding the received signal $r(t)$. Here, we utilized a dispersive five-path Gaussian channel, written as

$$h(t) = \sqrt{0.45}\delta(t) + 0.5\delta(t-T) + \sqrt{0.15}\delta(t-2T) + \sqrt{0.1}\delta(t-3T) + \sqrt{0.05}\delta(t-4T) \quad (1)$$

and a five-path, symbol-spaced fading channel of equal CIR weights

$$h(t) = \sum_{n=0}^{4} \sqrt{0.2} A_n \delta(t-nT)$$
$$E\left\{|A_n|^2\right\} = 1; \quad n = 0, \ldots, 4 \quad (2)$$

where A_n is a complex variable possessing Rayleigh fading statistics and obeys a normalized Doppler frequency of 1.5×10^{-4}. The resultant received signal $r(t)$ is:

$$r(t) = s(t) * h(t) + n(t) \quad (3)$$

where $*$ denotes convolution.

At the receiver, the CIR is estimated using an iterative CIR estimation technique [16], [17]. In the first turbo equalization iteration, the CIR is estimated using the least mean square (LMS) algorithm [18] and the training sequence mentioned previously. The initial step-size of the LMS algorithm is set to 0.05. Subsequently, the CIR estimate is then utilized by the soft-in/soft-out (SISO) [19] equalizer, which generates soft decisions in the form of the logarithmic probability ratios known as log-likelihood ratios (LLR). These soft decisions are passed to the channel decoder, which computes the reliability information referred to as *a posteriori* information, corresponding to the coded bits. At the next iteration, in addition to using the training sequences for reestimating the CIR, the soft estimates of the entire transmission burst's symbols derived from the *a posteriori* information of the SISO decoder are employed. Here, a smaller step-size of 0.01 is utilized in the LMS algorithm. The decoder's *a posteriori* information is transformed from the ratio of probability values into soft estimates of the modulated symbols by computing the statistical average of the transmitted symbol probabilities [20]. This CIR estimation process is repeated for each turbo equalization iteration.

Although there exists a wide range of low complexity SISO [19] algorithms, we have chosen the logarithmic-maximum *a posteriori* (Log-MAP) algorithm [21], [22] for the SISO channel equalizer and channel decoder, since the Log-MAP algorithm achieves optimal performance, despite having reduced computational complexity compared with the original maximum *a posteriori* (MAP) algorithm [23].

III. Overview of Turbo Equalization

Before proceeding with the overview of turbo equalization, let us first define the terms *a priori*, *a posteriori*, and extrinsic information. The *a priori* information associated with a bit is the information known before equalization or decoding commences, and originates from a source other than the received information or the code constraints. Next, the extrinsic information associated with a bit is defined as the information provided by the equalizer or decoder based on the received sequence and on the *a priori* information of all other bits with the exception of the received and *a priori* information explicitly related to that particular bit. Finally, the *a posteriori* information associated with a bit is the reliability information that the SISO algorithm provides taking into account *all* available sources of information about the particular bit.

As shown in Fig. 2, the turbo equalizer consists of a SISO equalizer and a SISO decoder. The SISO equalizer in Fig. 2 generates the *a posteriori* probability upon receiving the corrupted transmitted signal sequence and the *a priori* probability provided by the SISO decoder. However, at the initial iteration stages, i.e., at the first turbo equalization iteration, no *a priori* information is available. Therefore, the *a priori* probability is set to 1/2, since the transmitted bits are assumed to be equiprobable. Before passing the *a posteriori* information generated by the SISO equalizer to the SISO decoder of Fig. 2, the contribution

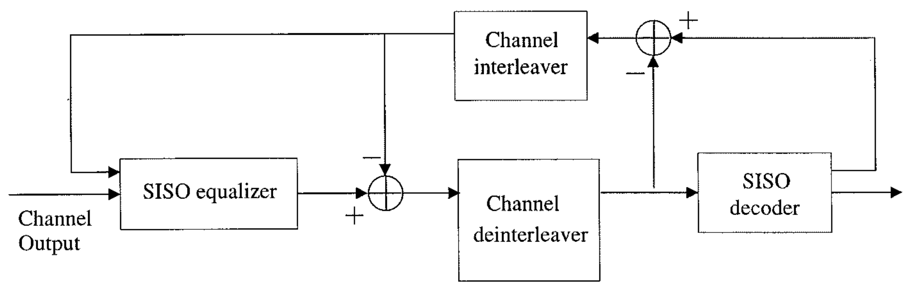

Fig. 2. Structure of original turbo equalizer introduced by Douillard *et al.* [1].

of the decoder, i.e., the *a priori* information accruing from the previous iteration must be removed, in order to yield the combined channel and extrinsic information. This also minimizes the correlation between the *a priori* information supplied by the decoder and the *a posteriori* information generated by the equalizer. The removal of the *a priori* information is necessary, in order to prevent the decoder from "reprocessing" its own information, which would result in the so-called "positive feedback" phenomenon, overwhelming the decoder's current reliability estimation of the coded bits, i.e., the extrinsic information.

The combined channel and extrinsic information is channel-deinterleaved and directed to the SISO decoder, as depicted in Fig. 2. Subsequently, the SISO decoder computes the *a posteriori* probability of the coded bits. Note that in contrast to turbo decoding, the SISO decoder of the turbo equalizer not only produces the *a posteriori* probability of the source bits, but also those of all channel coded bits. The deinterleaved channel and extrinsic information is then removed from the *a posteriori* information provided by the decoder in Fig. 2 before channel interleaving, in order to yield the extrinsic information. This is to prevent the channel equalizer from receiving information based on its own decisions, which was generated in the previous turbo equalization iteration. The interleaved extrinsic information computed is then employed as the *a priori* input information of the equalizer in the next channel equalization process. This constitutes the first turbo equalization iteration. The iterative process is repeated, until the required termination criteria are met [3]. At this stage, the *a posteriori* information of the source bits, which has been generated by the decoder is utilized to estimate the transmitted bits. Further discussions on turbo equalization/detection can be found in [1], [2], [8], and [24].

IV. Complexity of the Turbo Equalizers (TEQ)

This section presents the complexity of the TEQ utilized by the investigated systems. In order to simplify the complexity analysis of these systems, the complexity of the channel encoder, modulator, interleaver, and deinterleaver has been assumed to be negligible. Therefore, the complexity of the turbo equalizer is dependent only on the complexity of the equalizer, the decoder, and the number of turbo equalization iterations performed.

In order to determine the complexity of the turbo equalizer, the complexity of the equalizer and decoder is added and subsequently multiplied by the number of turbo equalization iterations. Therefore, we must adopt the same measure of complexity for both the equalizer and decoder, which in this paper is the number of associated trellis transitions per information bit. Since the complexity of the equalizer is dependent on the number of trellis transitions per coded bit, it must be normalized to become the number of transitions per information bit. This is achieved by multiplying the number of equalizer transitions per coded bit with the reciprocal of the code rate employed. For a BPSK equalizer, the number of transitions per coded bit depends on the number of trellis states and the number of trellis branches leaving each trellis state, as expressed below

$$\begin{aligned}\text{no. of transitions per coded bit} =& \text{no. of states} \times \text{no. of branches}\\ =& 2^L \times 2 = 2^{L+1}\end{aligned} \tag{4}$$

where L is the duration of the channel memory. Consequently, the number of trellis transitions per information data bit which is also proportional to the complexity $\mathrm{comp}[EQ]$ of the equalizer, can be expressed as

$$\begin{aligned}\mathrm{comp}[EQ] \propto& \frac{\text{no. of transitions per coded bit}}{\text{Code rate}}\\ \propto& \frac{2^{L+1}}{\text{Code rate}}.\end{aligned} \tag{5}$$

Let us now consider the complexity of the decoder. As mentioned above, the complexity of the decoder is dependent on the number of transitions considered for decoding each information data bit. Hence, for the convolutional decoder, the complexity $\mathrm{comp}[CC(2,1,K)]$ incurred is

$$\begin{aligned}\mathrm{comp}[CC(2,1,K)] \propto& \text{no. of states} \times \text{no. of branches}\\ \propto& 2^{K-1} \times 2 = 2^K\end{aligned} \tag{6}$$

since the convolutional code is a binary code which has two branches leaving each state.

For the convolutional turbo code, the complexity is a factor of two higher than that of the convolutional code $\mathrm{comp}[CC(2,1,K)]$, since the turbo decoder consists of two convolutional decoders. Therefore, the complexity $\mathrm{comp}[TC(2,1,K)]$ of the convolutional turbo code is written as

$$\begin{aligned}\mathrm{comp}[TC(2,1,K)] \propto& 2 \times \text{no. of states} \times \text{no. of branches}\\ \propto& 2 \times 2^{K-1} \times 2 = 2^{K+1}.\end{aligned} \tag{7}$$

As for BCH turbo codes, the number of transitions computed for each information bit varies depending on the specific segment of the decoding trellis considered, unlike for the convolutional decoder and for the convolutional turbo decoder. The decoding trellis of the $\mathrm{BCH}(n,k)$ code can be divided into three segments [25]. For every trellis instant q the number of states is given as [25]

$$\text{no. of States }(q) = \begin{cases} 2^q, & q = 0, 1, \ldots, n-k-1 \\ 2^{n-k}, & q = n-k, n-k+1, \ldots, k \\ 2^{n-q}, & q = k+1, k+2, \ldots, n. \end{cases} \quad (8)$$

Therefore, in order to determine the number of transitions computed for each information bit, the total number of transitions in the trellis must be calculated and subsequently divided by the total number of information bits. With the aid of the equations given below

$$2^{n-k} - 1 = \sum_{q=0}^{n-k-1} 2^q \quad (9)$$

$$= \sum_{q=k+1}^{n} 2^{n-q} \quad (10)$$

we can determine the number of transitions for each of the three decoding trellis segments. Starting with the segment where $q = 0, \ldots, n-k-1$, we note that the total number of states is $\sum_{q=0}^{n-k-1} 2^q$, which from (9) is equal to $2^{n-k} - 1$. Therefore, the total number of transitions is $(2^{n-k} - 1) \times 2$. Using (8), the total number of states in segment $q = n-k, \ldots, k$ is $(2k - n + 1) \times 2^{n-k}$. However, since the trellis begins to converge back to the all-zero state for $q > k$, the total number of transitions in this segment is $(2k - n) \times 2^{n-k} \times 2$. Finally, by using (10), the total number of transitions for the segment, where $k+1, \ldots, n$, is $\left(\sum_{q=k+1}^{n} 2^{n-q}\right) \times 2 = (2^{n-k} - 1) \times 2$. By summing the number of transitions for each of the three trellis segments, we obtain the total number of transitions for the entire decoding trellis. Hence, the number of transitions per information bit which is also our measure of the complexity for BCH turbo codes, $\mathrm{comp}[\mathrm{TBCH}(n,k)]$ becomes

$$\begin{aligned} &\mathrm{comp}[\mathrm{TBCH}(n,k)] \\ &\quad \propto 2 \times \frac{\text{Total no. of transitions}}{k} \\ &\quad \propto 2 \times \frac{\left[2 \times (2^{n-k} - 1) + (2k-n) \times 2^{n-k}\right] \times 2}{k}. \end{aligned} \quad (11)$$

As in the case of the convolutional turbo codes in (7), a multiplicative factor of two was applied, since there are two component BCH decoders in the turbo decoder.

Having determined the complexity of the equalizer and decoder as a function of the number of transitions per information bit, the complexity $\mathrm{comp}[\mathrm{TEQ}]$ of the turbo equalizer can be expressed as

$$\begin{aligned} \mathrm{comp}[\mathrm{TEQ}] \propto (&\mathrm{comp}[EQ] + \text{Decoder complexity}) \\ &\times \text{no. of TEQ iterations}. \end{aligned} \quad (12)$$

Using (6), (7), (11), and (12), the complexity of the turbo equalizers was evaluated and summarized in Table I.

V. Simulation Parameters

In this contribution, BPSK modulation is employed in all the examined systems. The first system described is a convolutional-coded scheme, denoted by CC. A rate $R = 1/2$, constraint length $K = 5$, nonrecursive convolutional code was used with octal generator polynomials $G_0 = 35$ and $G_1 = 23$. In order to obtain $R = 3/4$ and $R = 5/6$ rate convolutional codes, we have employed the puncturing pattern used by Yasuda *et al.*, which is specified in Table II.

For the convolutional turbo-coded system, represented by CT, we have used the rate $R = 1/2, K = 3$ convolutional constituent codes employing the feedback generator polynomial of $G_0 = 7$ and feedforward polynomial of $G_1 = 5$. A constraint length of $K = 3$ was employed for the convolutional turbo codes, in order to obtain a fair comparison with the similar-complexity $K = 5$ convolutional codes. When no puncturing is implemented, the overall rate of the turbo code is $R = 1/3$. Therefore, we have applied regular puncturing as detailed in Table III, to the turbo codes

TABLE I
TABLE OF TURBO EQUALIZER COMPLEXITY OF THE CC, CT, AND BT SYSTEMS FOR CODE RATES OF $R \approx 1/2$, $R \approx 3/4$, AND $R \approx 5/6$. THE CHANNEL MEMORY L FOR BOTH THE FIVE-PATH GAUSSIAN CHANNEL AND FIVE-PATH RAYLEIGH FADING CHANNEL IS EQUAL TO FOUR

Code	No. of Iterations		Relative complexity	
	Static channel	Fading channel	Static channel	Fading channel
Convolutional Code (CC)				
$R = 1/2$ $K = 5$ CC	6	3	576	288
$R = 3/4$ $K = 5$ CC	8	3	597	224
$R = 5/6$ $K = 5$ CC	6	3	422	211
Convolutional Turbo Code (CT)				
$R = 1/2$ $K = 3$ CT	6	8	480	640
$R = 3/4$ $K = 3$ CT	8	8	469	469
$R = 5/6$ $K = 3$ CT	6	8	326	435
BCH Turbo Code (BT)				
$R = 11/19$ BCH(15,11)	8	6	854	641
$R = 26/36$ BCH(31,26)	6	6	944	944
$R = 57/69$ BCH(63,57)	4	6	1106	1660

TABLE II
PUNCTURING PATTERN [26] APPLIED TO THE CODED BITS OF THE $R = 1/2$ CONVOLUTIONAL CODE IN ORDER TO OBTAIN CODE RATES $R = 3/4$ AND $R = 5/6$ CONVOLUTIONAL CODES

Code Rate $R = \frac{3}{4}$	Code Rate $R = \frac{5}{6}$
G_0: 1 1 0	G_0: 1 1 0 0 0
G_1: 1 0 1	G_1: 1 0 1 1 1

1 = transmitted bit

0 = non transmitted bit

TABLE III
REGULAR PUNCTURING PATTERN USED IN ORDER TO OBTAIN THE $R = 1/2$, $R = 3/4$, AND $R = 5/6$ CONVOLUTIONAL TURBO CODES. THE TERMS $C1$ AND $C2$ REPRESENT THE PARITY BITS OF $R = 1/2$ CONVOLUTIONAL CODES OF THE FIRST AND SECOND CONSTITUENT CODES, RESPECTIVELY

Code Rate $R = \frac{1}{2}$	Code Rate $R = \frac{3}{4}$	Code Rate $R = \frac{5}{6}$
C1: 1 0	C1: 1 0 0 0 0 0 0 0 1 0 0 0	C1: 1 0 0 0 0 0 0 0 0 0
C2: 0 1	C2: 0 0 1 0 0 0 0 0 0 0 1 0	C2: 0 0 0 0 1 0 0 0 0 0

1 = transmitted bit

0 = non transmitted bit

TABLE IV
SIZE OF RANDOM CHANNEL AND CODING INTERLEAVERS USED IN THE $R \approx 1/2$, $R \approx 3/4$, AND $R \approx 5/6$-RATE BPSK, CC, CT AND BT SYSTEMS

Random channel interleaver size					
$R=\frac{1}{2}$ **CC/CT**	$R=\frac{3}{4}$ **CC/CT**	$R=\frac{5}{6}$ **CC/CT**	$R=\frac{11}{19}$ **BT**	$R=\frac{26}{36}$ **BT**	$R=\frac{57}{69}$ **BT**
20736	20736	20736	21888	20736	19872
Random coding interleaver size					
$R=\frac{1}{2}$ **CT**	$R=\frac{3}{4}$ **CT**	$R=\frac{5}{6}$ **CT**	$R=\frac{11}{19}$ **BT**	$R=\frac{26}{36}$ **BT**	$R=\frac{57}{69}$ **BT**
10368	15552	17280	12672	14976	16416

in order to obtain $R=1/2$, $R=3/4$, and $R=5/6$ rate convolutional turbo codes. Note that the puncturing patterns employed in these systems have been determined experimentally. For procedures on designing optimum high-rate turbo codes via puncturing, the interested reader is referred to [12].

Finally, for the BCH turbo-coded system which we denoted by BT, three different constituent BCH codes were used, namely the BCH(15,11) code, the BCH(31,26) code, and the BCH(63,57) code in order to obtain the code rates of $R=11/19$, $R=26/36$, and $R=57/69$, respectively. No puncturing is required for this class of turbo codes.

We used a random channel interleaver, which was employed in the original turbo equalizer proposed by Douillard *et al.* [1], for all three turbo equalization systems and the interleaver size was set to approximately 20 000 bits. Similarly, random turbo coding interleavers were used in the turbo equalizers employing BCH turbo codes and convolutional turbo codes. Note that the same random interleaver mapping rules were used throughout the simulation. The detailed channel and turbo coding interleaver sizes are specified in Table IV. The number of turbo equalization iterations performed is specified in Table I. Here, the required number of iterations was determined experimentally and it was defined as the number of iterations, beyond which yielded no significant iteration gains. A total of 5×10^6 bits were transmitted for each signal-to-noise ratio (SNR) value in our investigations.

Our comparative study was conducted both over a five-path Gaussian channel, which is given in (1) and an equally-weighted five-path Rayleigh fading channel, as shown in (2), using a normalized Doppler frequency of $f_d = 1.5 \times 10^{-4}$. Note that for a fixed information rate, the channel ISI pattern will vary for different code rates. Therefore, in order to achieve a fair comparison, the performance of the turbo equalizer must be compared for a particular code rate, but not between different code rates.

As mentioned in Section II, we have employed the iterative CIR estimation technique proposed in [16]. Our simulations demonstrated that the performance of the turbo equalizer using the iterative CIR estimator was virtually the same as that of the turbo equalizer possessing perfect CIR knowledge after performing the critical number of turbo equalization iterations. Therefore, in our contribution the simulation results obtained using the iterative CIR estimator also closely represent the performance of the turbo equalizer possessing perfect CIR knowledge.

VI. RESULTS AND DISCUSSION

In this section, we compared the turbo equalization performance of the CC, CT, and BT systems investigated. We commence by comparing the turbo equalization performance of the CT, BT, and CC systems for code rates of $R \approx 1/2$, $R \approx 3/4$, and $R \approx 5/6$ over the five-path Gaussian channel, followed by the five-path Rayleigh fading channel results in (1) and (2), respectively. We have compared the performance of these schemes at the target BER of 10^{-3}, noting that a similar preference order has been observed at the BERs of 10^{-4} and 10^{-5} for the various schemes. We also note that the performance of the coded systems recorded for transmission over the nondispersive AWGN channel was included in both Figs. 3 and 4 for comparison.

A. Five-Path Gaussian Channel

Fig. 3(a) shows the turbo equalization performance of the $R=11/19$ BT system, the $R=1/2$ CT system, and the $R=1/2$ CC system over the five-path Gaussian channel shown in (1). At $\mathrm{BER}=10^{-3}$, we observed that the performance of the $R=1/2$ CT system was comparable to the $R=1/2$ CC system. Both of these systems outperformed the $R=11/19$ BT system by approximately 1.0 dB at $\mathrm{BER}=10^{-3}$. The same comparison was performed for $R \approx 3/4$ BPSK turbo equalizers in Fig. 3(b). We observed that the performance of the $R=3/4$ CT scheme was again comparable to the $R=3/4$ CC system, while achieving a gain of 0.7 dB over the $R=26/36$ BT system at $\mathrm{BER}=10^{-3}$. Fig. 3(c) shows the turbo equalization performance of the $R=57/69$ BT system, the $R=5/6$ CT scheme, and that of the $R=5/6$ CC system. For this code rate, we observed that the $R=5/6$ CT system achieved a gain of 0.8 dB over the $R=57/69$ BT system at $\mathrm{BER}=10^{-3}$ and was comparable to the $R=5/6$ CC system. The results demonstrated that at high code rates and for transmission over the dispersive Gaussian channel of (1) turbo equalizers using convolutional turbo codes and convolutional codes required similar E_b/N_o values in order to achieve a BER of 10^{-3}. It was also observed that both of these systems achieved gains of 0.7 dB–1.0 dB, when compared with the BT schemes.

B. Equally Weighted Five-Path Rayleigh Fading Channel

Let us now compare the turbo equalization performance of the CC, CT, and BT systems, for particular code rates of $R \approx 1/2$, $R \approx 3/4$, and $R \approx 5/6$ over the five-path Rayleigh fading

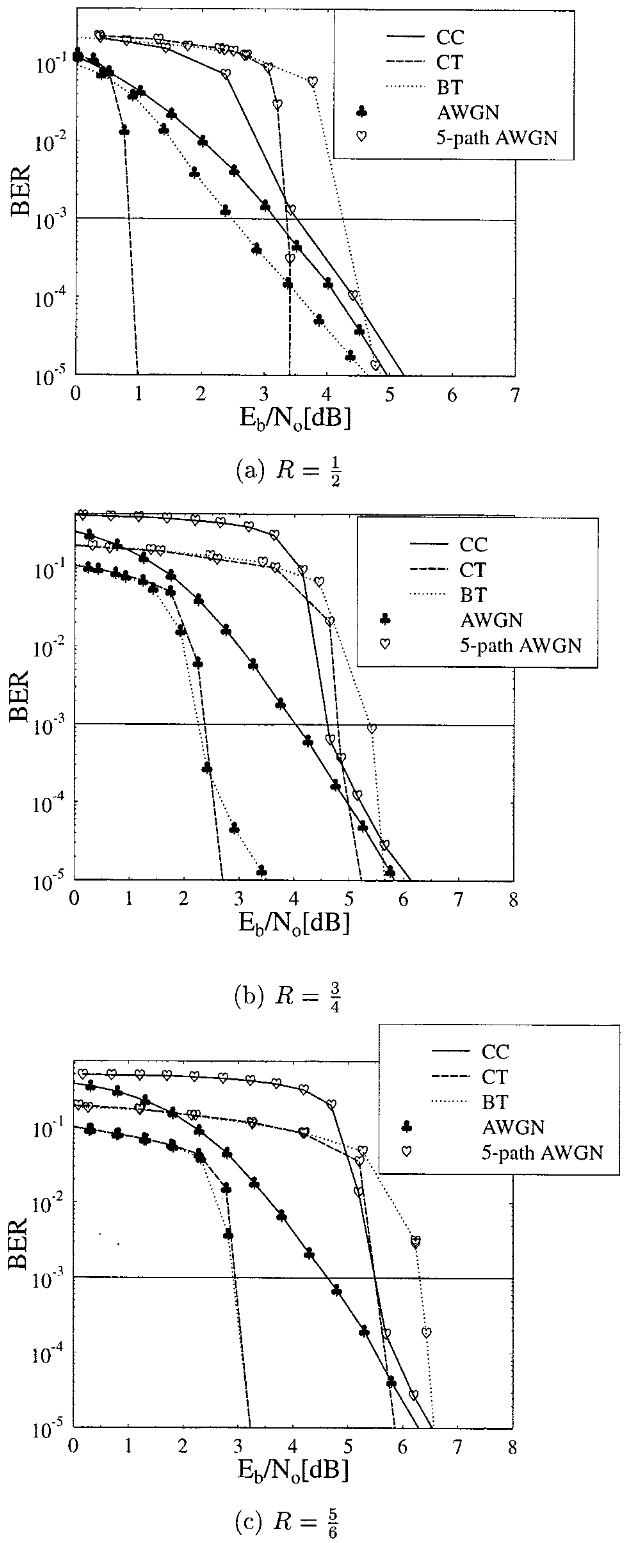

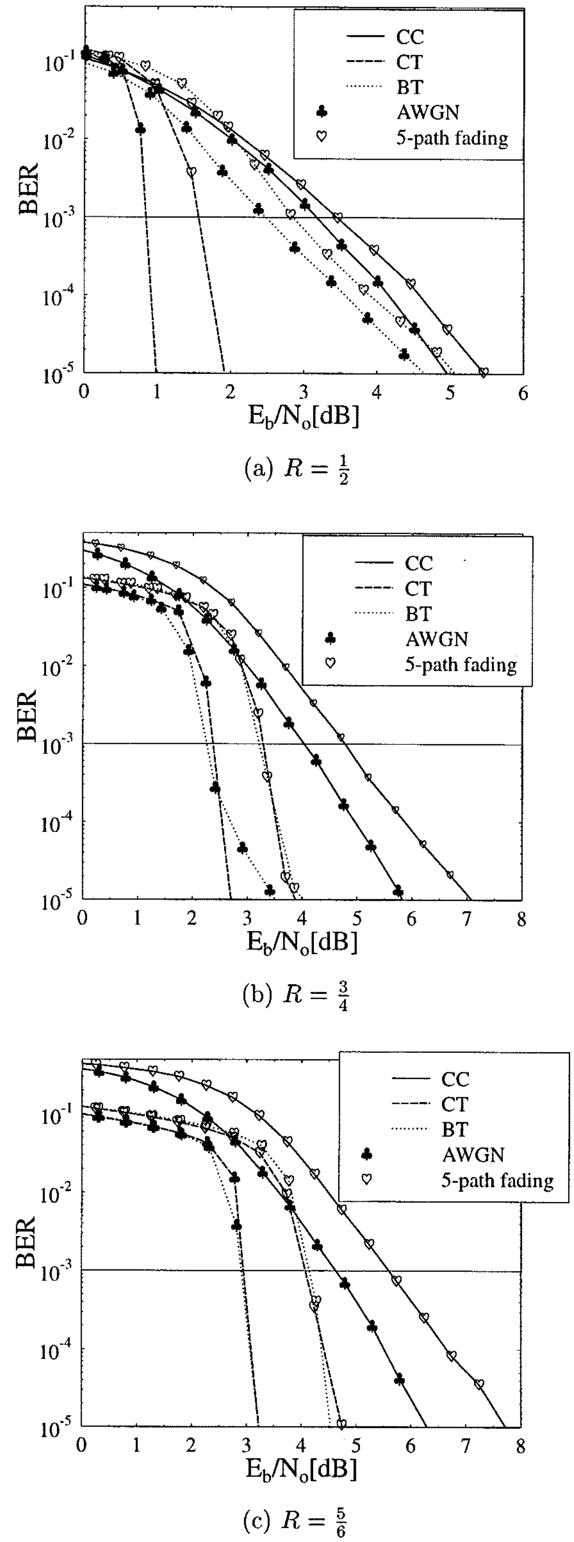

Fig. 3. Comparing the turbo equalization performance of the CC system, the CT scheme, and the BT system for code rates $R = 1/2$, $R = 3/4$, and $R = 5/6$ over the **five-path Gaussian channel** of (1).

Fig. 4. Comparing the turbo equalization performance of the CC system, the CT scheme, and the BT system for code rates $R = 1/2$, $R = 3/4$, and $R = 5/6$ over the **five-path Rayleigh fading channel** of Fig. 2.

channel shown in (2). As shown in Fig. 4(a), the $R = 1/2$ CT system achieved a gain of 1.6 dB and 1.9 dB, when compared with the $R = 11/19$ BT system and the $R = 1/2$ CC system at $\mathrm{BER} = 10^{-3}$. For a code rate of $R \approx 3/4$, we observed in Fig. 4(b) that the BT system and the CT scheme required a similar E_b/N_o value in order to achieve $\mathrm{BER} = 10^{-3}$. Relative to the BT system and the CT scheme, the CC system exhibited an E_b/N_o loss of 1.4 dB at $\mathrm{BER} = 10^{-3}$. The same performance trend was observed in Fig. 4(c) for the $R \approx 5/6$ rate turbo equalizers, where the BT system and CT scheme required a similar E_b/N_o in order to achieve a $\mathrm{BER} = 10^{-3}$. Both systems obtained a gain of 1.5 dB at $\mathrm{BER} = 10^{-3}$ when compared with the $R = 5/6$ rate CC system. Over the Rayleigh fading channel, the CT system was again the best, achieving better performance than the CC system. When compared with the BT schemes, the rate $R = 1/2$ CT system outperformed the $R = 11/19$ BT system, while the rate $R = 3/4$ and $R = 5/6$ CT systems were comparable to the performance of the $R = 26/36$ and $R = 57/69$ BT systems.

In the five-path Gaussian channel, the performance of the high-code-rate CT system was comparable to the CC system and outperformed the BT scheme at $\mathrm{BER} = 10^{-3}$. For the five-path Rayleigh fading channel scenario, the performance of the $R = 1/2$ CT system is better, than that of the other systems of similar code rate. However, for higher code rates, its performance is similar to that of the BT system at $\mathrm{BER} = 10^{-3}$. Still, the CT system is favored as it is computationally less complex than the BT scheme (see Table I).

It was also observed in Fig. 4(a)–(c) that the CC turbo equalizer systems required only three turbo equalization iterations over the five-path Rayleigh fading channel for all code rates. Furthermore, the CC schemes were seen to perform poorly over the Rayleigh fading channel. For example, for a code rate of $R \approx 5/6$ and at $\mathrm{BER} = 10^{-3}$, a loss of 1.5 dB was observed, when compared with the turbo-equalized CT system. A reason for this marginal improvement of the CC scheme through iterative equalization and decoding is that the CC system's performance is already close to the optimum, i.e., only 1.1 dB from the decoding performance over the nondispersive Gaussian channel, after three iterations.

It was also observed that the performance of the turbo-equalized CC systems transmitting over the dispersive Gaussian and Rayleigh fading channels of (1) and (2), respectively, approach the nondispersive AWGN performance. This trend was also seen for the turbo-coded CT and BT schemes transmitting over the dispersive Rayleigh fading channel. However, over the dispersive Gaussian channel the performance of the high-rate CT and BT coded turbo-equalized systems was approximately 2.5 dB–3.0 dB poorer than their corresponding AWGN performance. It is worth noting that the gap between the nondispersive AWGN channel performance and the turbo-equalized CT performance curve of the five-path dispersive Gaussian channel is due to the fact that the turbo equalizer is required to operate and to converge under extremely low SNR conditions. In this low-SNR region, the powerful turbo decoder used over the nondispersive AWGN channel is capable of providing a good performance, whereas the turbo equalizer is unable to converge when communicating over the five-path dispersive Gaussian channel resulting in the above-mentioned 2.5 dB–3.0 dB performance gap. In contrast to turbo codes, convolutional codes exhibit an inferior performance, hence, they require a higher operating SNR over nondispersive Gaussian channels and in this higher SNR region the turbo equalizer exhibits better convergence properties. This is why the performance gap between the CC nondispersive AWGN channel scenario and the turbo-equalized dispersive five-path Gaussian channel scenario appears more narrow, than for the corresponding turbo-coded scenario.[1]

[1]The authors wish to thank the reviewer for the above observation.

VII. Conclusion

The turbo equalization performance of BPSK modulated transmission systems using BCH turbo codes, convolutional turbo codes, and convolutional codes was compared at code rates of $R \approx 1/2$, $R \approx 3/4$ and $R \approx 5/6$. Our comparative study of the turbo equalizers showed that for the five-path Gaussian channel of (1) and at high code rates of $R \approx 3/4$ and $R \approx 5/6$, the convolutional turbo coded system CT yielded better performance, when compared with the BCH turbo coded BT system and gave comparable performance to the convolutional-coded system CC at $\mathrm{BER} = 10^{-3}$. Furthermore, this performance was obtained by the CT scheme at the lowest complexity as compared with that of the BT and CC systems. Over the equally-weighted symbol-spaced five-path Rayleigh fading channel of Fig. 2, the CT system was again the best, achieving better performance than the CC system. When compared with the BT schemes, the rate $R = 1/2$ CT system outperformed the $R = 11/19$ BT system, while the rate $R = 3/4$ and $R = 5/6$ CT systems were comparable to the performance of the $R = 26/36$ and $R = 57/69$ BT systems. It was also observed that the CC turbo equalizer system performed poorly and required only three turbo equalization iterations, whereas the turbo-coded turbo equalizer schemes needed six to eight iterations. This was because after three iterations the performance of the CC system was already close to the decoding results over the nondispersive Gaussian channel. On the whole, the turbo-equalized CT system was the most robust scheme, giving better or comparable performance for all code rates investigated. Furthermore, the CT system incurs moderate computational complexity compared with the other schemes, hence, it constitutes the best choice in most turbo equalizer applications.

Acknowledgment

We are also grateful for the insightful and constructive comments of the reviewers.

References

[1] C. Douillard, A. Picart, M. Jézéquel, P. Didier, C. Berrou, and A. Glavieux, "Iterative correction of intersymbol interference: Turbo-equalization," *Eur. Trans. Commun.*, vol. 6, pp. 507–511, Sept.–Oct. 1995.

[2] M. J. Gertsman and J. L. Lodge, "Symbol-by-symbol MAP demodulation of CPM and PSK signals on Rayleigh flat-fading channels," *IEEE Trans. Commun.*, vol. 45, pp. 788–799, July 1997.

[3] G. Bauch, H. Khorram, and J. Hagenauer, "Iterative equalization and decoding in mobile communications systems," in *Proc. the European Personal Mobile Communications Conf.*, Bonn, Germany, Sept. 30–Oct. 2 1997, pp. 301–312.

[4] M. Moher, "Decoding via cross-entropy minimization," in *Proc. IEEE Global Telecommunications Conf. 1993*, Houston, TX, Nov. 29 –Dec. 2 1993, pp. 809–813.

[5] G. Bauch and V. Franz, "Iterative equalization and decoding for the GSM-system," in *Proc. IEEE 48th Vehicular Technology Conf.*, Ottawa, Canada, May 18–21, 1998, pp. 2262–2266.

[6] C. Berrou, A. Glavieux, and P. Thitimajshima, "Near Shannon limit error-correcting coding and decoding: Turbo codes," in *Proc. Int. Conf. Communications*, Geneva, Switzerland, May 23–26, 1993, pp. 1064–1070.

[7] C. Berrou and A. Glavieux, "Near optimum error-correcting coding and decoding: Turbo codes," *IEEE Trans. Commun.*, vol. 44, pp. 1261–1271, Oct. 1996.

[8] D. Raphaeli and Y. Zarai, "Combined turbo equalization and turbo decoding," in *Proc. Global Telecommunications Conf. 1997*, Phoenix, AZ, Nov. 3–8, 1997, pp. 639–641.

[9] T. Souvignier, A. Friedman, M.Öberg, R. E. S. P. H. Siegel, and J. Wolf, "Turbo decoding for pr4: Parallel versus serial concatenation," in *Proc. Int. Conf. Communications 1999*, Vancouver, Canada, June 6–10, 1999, pp. 1638–1642.

[10] J. Hagenauer, E. Offer, and L. Papke, "Iterative decoding of binary block and convolutional codes," *IEEE Trans. Inform. Theory*, vol. 42, pp. 429–445, Mar. 1996.

[11] H. Nickl, J. Hagenauer, and F. Burkett, "Approaching Shannon's capacity limit by 0.27 dB using simple hamming codes," *IEEE Commun. Lett.*, vol. 1, pp. 130–132, Sept. 1997.

[12] Ö. F. Açikel and W. E. Ryan, "Punctured turbo-codes for BPSK/QPSK channels," *IEEE Trans. Commun.*, vol. 47, pp. 1315–1323, Sept. 1999.

[13] A. Hocquenghem, "Codes correcteurs d'erreurs," *Chiffres (Paris)*, vol. 2, pp. 147–156, Sept. 1959.

[14] R. C. Bose and D. K. Ray-Chaudhuri, "On a class of error-correcting binary group codes," *Inf. Control*, vol. 3, pp. 68–79, Mar. 1960.

[15] A. Klein, R. Pirhonen, J. Sköld, and R. Suoranta, "FRAMES multiple access model—Wideband TDMA with and without spreading," in *Proc. IEEE Int. Symp. Personal, Indoor, and Mobile Radio Communications 1997*, Helsinki, Finland, Sept. 1–4, 1997, pp. 37–41.

[16] C. H. Wong, B. L. Yeap, and L. Hanzo, "Wideband burst-by-burst adaptive modulation with turbo equalization and iterative channel estimation," in *Proc. IEEE Vehicular Technology Conf. 2000*, Tokyo, Japan, May 15–18, 2000, pp. 2044–2048.

[17] M. Sandell, C. Luschi, P. Strauch, and R. Yan, "Iterative channel estimation using soft decision feedback," in *Proc. Global Telecommunications Conf. 1998*, Sydney, Australia, Nov. 8–12, 1998, pp. 3728–3733.

[18] S. Haykin, *Adaptive Filter Theory*. Englewood Cliffs, NJ: Prentice-Hall, 1996.

[19] S. Benedetto, D. Divsalar, G. Montorsi, and F. Pollara, "A soft-input soft-output APP module for iterative decoding of concatenated codes," *IEEE Commun. Lett.*, vol. 1, pp. 22–24, Jan. 1997.

[20] A. Glavieux, C. Laot, and J. Labat, "Turbo equalization over a frequency selective channel," in *Proc. Int. Symp. Turbo Codes, and Related Topics*, Brest, France, Sept. 3–5, 1997, pp. 96–102.

[21] P. Robertson, E. Villebrun, and P. Hoeher, "A comparison of optimal and sub-optimal MAP decoding algorithms operating in the log domain," in *Proc. Int. Conf. Communications*, Seattle, WA, June 18–22, 1995, pp. 1009–1013.

[22] P. Robertson, P. Hoeher, and E. Villebrun, "Optimal and sub-optimal maximum a posteriori algorithms suitable for turbo decoding," *Eur. Trans. Telecommun.*, vol. 8, pp. 119–125, Mar./Apr. 1997.

[23] L. R. Bahl, J. Cocke, F. Jelinek, and J. Raviv, "Optimal decoding of linear codes for minimizing symbol error rate," *IEEE Trans. Inform. Theory*, pp. 284–287, Mar. 1974.

[24] S. Benedetto, D. Divsalar, G. Montorsi, and F. Pollara, "Serial concatenation of interleaved codes: Performance analysis, design, and iterative decoding," *IEEE Trans. Inform. Theory*, vol. 44, pp. 909–926, May 1998.

[25] J. Wolf, "Efficient maximum likelihood decoding of linear block codes using a trellis," *IEEE Trans. Inform. Theory*, vol. 24, pp. 76–80, Jan. 1978.

[26] Y. Yasuda, K. Kashiki, and Y. Hirata, "High-rate punctured convolutional codes for soft decision Viterbi decoding," *IEEE Trans. Commun.*, vol. COM-32, pp. 315–319, Mar. 1984.

[27] L. Hanzo, T. H.. Liew, and B. L. Yeap, *Turbo-Coding, Turbo-Equalization and Space–Time Coding*. New York: Wiley, 2002.

Bee Leong Yeap received the B.Eng. (honors) degree in electronics engineering from the University of Southampton, U.K., in 1996. In 2000, he received the Ph.D. degree.

Since then, he has been continuing his research as a Postdoctoral Research Fellow at the University of Southampton. His research interests include turbo coding, turbo equalization, adaptive modulation, and space–time coding.

Tong Hooi Liew received the B.Eng. degree in electronics engineering from the University of Southampton, U.K. He also received the Ph.D. degree.

Currently, he is continuing his research as a Postdoctoral Research Fellow. His current research interests include coding and modulation for wireless channels, space–time coding, adaptive transceivers, etc. He has published his research results widely.

J. Hámorský, photograph and biography not available at the time of publication.

Lajos Hanzo (SM'92) received the B.Eng. degree in electronics, in 1976, and received the Ph.D. degree, in 1983.

He has held various research and academic posts in Hungary, Germany, and the U.K. during his 25-year career in telecommunications. Since 1986, he has been with the Department of Electronics and Computer Science, University of Southampton, U.K., and has been a Consultant to Multiple Access Communications Ltd., U.K. Currently, he holds the Chair in Telecommunications. He has co-authored eight books on mobile radio communications, published about 400 research papers, organized and chaired conference sessions, presented overview lectures, and was awarded a number of distinctions. Currently, he is managing a research team, working on research projects in the field of wireless multimedia communications under the auspices of the Engineering and Physical Sciences Research Council (EPSRC) U.K., European IST Programme, and Mobile Virtual Center of Excellence (VCE). He provides industrial training courses

Dr. Hanzo is an IEEE distinguished lecturer.